Reflectance difference spectroscopy of GaAs(001) under a [110] uniaxial stress

L. F. Lastras-Martínez,[1,*] M. Chavira-Rodríguez,[1] R. E. Balderas-Navarro,[1,2] J. M. Flores-Camacho,[1] and A. Lastras-Martínez[1]

[1]*Instituto de Investigación en Comunicación Optica, Universidad Autonóma de San Luis Potosí, Alvaro Obregón 64, San Luis Potosí, México*

[2]*Facultad de Ciencias, Universidad Autonóma de San Luis Potosí, Alvaro Obregón 64, San Luis Potosí, México*

(Received 3 February 2004; published 15 July 2004)

We report on reflectance-difference spectra of *n*-type GaAs(001) under a [110] uniaxial stress. Measurements where carried out in the energy range from 2.5−5.5 eV. This energy range comprises transitions E_1, $E_1+\Delta_1$, E_0', $E_0'+\Delta_0'$, $E_0'+\Delta_0'+\Delta_0$ and E_2. RD spectra shows sharp structures around 3.0 eV (E_1 and $E_1+\Delta_1$ transitions). Optical structure is also observed in the energy interval corresponding to the E_0'-triplet (4.4 −5.0 eV). Despite the fact that the E_2 transition dominates the GaAs reflectance spectrum around 5.0 eV, its contribution to the reflectance-difference (RD) spectra is found to be negligible. This fact was verified by polarized photoreflectance spectra. RD spectra are thus found to comprise only components associated to critical points of Λ and Γ symmetries. Furthermore, on the basis of a perturbative approach, we developed a theoretical RD line-shape model that shows an excellent agreement with experimental spectra. Results presented in this paper should probe to be useful in the identification of strain-related features in RD spectra and should contribute to the understanding of the different physical mechanisms leading to reflectance anisotropies.

DOI: 10.1103/PhysRevB.70.035306 PACS number(s): 78.20.−e, 78.66.−w, 78.90.+t

I. INTRODUCTION

Reflectance-difference spectroscopy (RDS) has emerged in the last two decades as a tool to study surface and interface anisotropies in zinc-blende semiconductors.[1,2] In (001)-oriented crystals RDS measures the difference in reflectivity between [110] and $[1\bar{1}0]$ light polarizations. For crystals of zinc-blende structure a polarization-independent reflectance spectrum may be expected from crystal symmetry considerations.[1] Therefore, any observed anisotropy must be associated to the region near the surface (or interface in the case of heterostructures) where the cubic symmetry has been broken.

One of the most important application of RDS regards the *in situ* monitoring of the epitaxial growth of zinc-blende semiconductors.[3,4] For these applications RDS offers advantages over other techniques due to its high sensitivity and experimental simplicity. Nevertheless, because the cubic symmetry may be broken for a number of physical mechanisms (surface reconstruction,[5–9] dislocations,[10–12] local field effects,[13] surface electric fields,[14] etc.), RD line shapes are prone to comprise more than one component, thus making their interpretation difficult. The lack of an adequate theoretical understanding of RD line shapes has limited the widespread use of RDS as an *in situ*, real time probe for epitaxial growth processes.

A reflectance anisotropy may also be induced by applying an external uniaxial stress along either [110] or $[1\bar{1}0]$. Such stress changes the zinc-blende symmetry from cubic to orthorhombic inducing a RDS signal that increases with applied stress strength. RDS measurements of GaAs, InP, and ZnSe under an uniaxal stress have demonstrated the high sensitivity of this spectroscopy for the determination of piezo-optical properties of cubic semiconductors.[15,16]

In this paper we report on the results of a research undertaken to determine the experimental RD line shape of GaAs(001) crystals under a [110] uniaxial stress, in the energy range from 2.5−5.5 eV. We further report on the development of a theoretical RD line shape that accurately describes the observed experimental spectrum. The investigated energy range comprises critical points of Λ, Γ, Δ, X, and Σ symmetries.[17,18] The applied stress, however, does not render Δ and X transitions anisotropic and thus they do not contribute to the RD line shape. Furthermore, it is found that Σ transitions are largely isotropic under the applied stress. The experimental line shapes in the energy range investigated in this paper are therefore found to comprise only contributions from critical points of Λ and Γ symmetries. Results reported here should prove to be useful in the identification of stress-related features in RD line shapes.

The rest of the paper is organized as follows: In Sec. II we discuss experimental details, in Sec. III we present experimental RD spectra, and in Sec. IV we develop the RDS theory for Λ and Γ critical points. Using this theory we fit the experimental results in Sec. V. Finally, conclusions are given in Sec. VI.

II. EXPERIMENTAL DETAILS

RDS measurements were carried out in air and at room temperature on *n*-type GaAs(001) crystals with a carrier concentration of $n=5.6\times10^{16}$ cm^{-3} that was cut from a commercial wafer with no further treatment. RD spectra were obtained in the energy range from 2.5−5.2 eV by using a setup described elsewhere.[19] A 75-W Xe lamp was employed as the light source and a silicon diode as the photodetector. The samples were cut out from commercial wafers in pieces $3.0\times3.0\times0.5$ mm in size. Crystal direction were determined by etching in (KOH).[20] RDS measurements were carried out by applying a stress along either [110] or $[1\bar{1}0]$ by

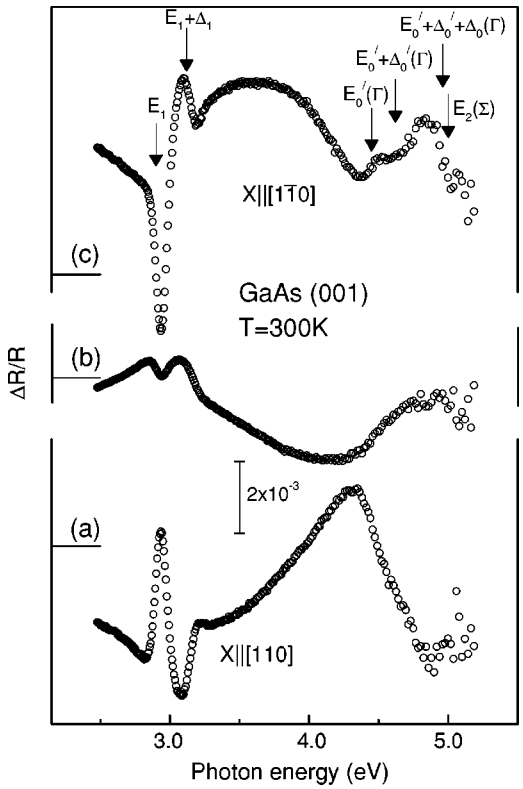

FIG. 1. RD room temperature spectra for (a) [110] uniaxial stress with magnitude -1.2×10^9 dyn/cm^2, (b) with no applied stress, and (c) [1$\bar{1}$0] uniaxial stress with magnitude -1.6×10^9 dyn/cm^2. Arrows indicate the energy positions for the interband GaAs bulk transitions.

using a calibrated spring. The experimental setup allowed us to apply stresses up to -5.0×10^9 dyn/cm^2. To get rid of any parasitic signal, two RD spectra were measured at each applied stress, at two azimuth angles 90° apart. The artifact-free signal was obtained by subtracting the two measured spectra.[19]

In order to model RD spectra, we measured the sample dielectric function by spectroscopic ellipsometry (SE) by using a rotating analyzer ellipsometer.[21] The measured pseudodielectric function $\langle\varepsilon\rangle$ was corrected for the presence of a GaAs oxide layer. The oxide thickness was determined by applying a three-phase (bulk-oxide-ambient) model,[22] assuming sharp interfaces and using literature data for the dielectric responses for GaAs[23] and GaAs oxide.[24] We found a thickness of 40 Å for the oxide layer.

III. EXPERIMENTAL RESULTS

Figure 1 shows experimental room temperature RD spectra for GaAs(001): (a) under strees along [110] with magnitude $X=-1.2\times10^9$ dyn/cm^2, (b) with no applied stress and (c) under stress along [1$\bar{1}$0] with magnitude $X=-1.6\times10^9$ dyn/cm^2. Spectra are shown in the range from 2.5 to 5.2 eV. As pointed out above, this photon energy range comprises transitions of Λ, Γ, Δ, X, and Σ symmetries. For a stress along [110] or [1$\bar{1}$0] the critical points of Δ and X symmetries do not contribute to reflectance anisotropy. This can be understood by considering that the projection of the stress perturbation is the same for all six vectors of the (100) family. Using similar arguments it is not difficult to see that only one-third of the Σ critical points could contribute to reflectance anisotropy. For Λ and Γ symmetry points, the perturbation along [110] splits the four-fold degenerate valence band and, in general, these points contribute to reflectance anisotropy.

The anisotropic transitions in the energy range investigated are E_1, $E_1+\Delta_1$ (Λ-symmetry), E_0', $E_0'+\Delta_0'$ and $E_0'+\Delta_0'+\Delta_0$ (Γ-symmetry), and E_2 (Σ-symmetry[25]). The energies for these transitions at room temperature are shown by arrows in Fig. 1. We note that E_0', $E_0'+\Delta_0'$ transitions are actually doublets involving Γ and Δ critical points. However, as pointed out above, only the Γ-symmetry components contribute to reflectance anisotropy.

We can see that the RD spectra of Fig. 1 display structures around transitions E_1, $E_1+\Delta_1$ and E_0'-triplet that reverse sign when rotating the applied stress direction from [110] to [1$\bar{1}$0] indicating that they have a linear-strain origin. We note, nevertheless, that the overall RD line shape does not simply change sign when rotating the applied stress. This is due to the fact that, besides the applied stress component, both RD spectra comprise an additional residual component. The residual component corresponds to the unstressed spectrum of Fig. 1(b).

We note that the residual RD spectrum shows around E_1 and $E_1+\Delta_1$ features similar to those of the stressed samples. This fact indicates the existence of internal orthorhombic strains associated to either a surface electric field.[26,27] or to 60° dislocations.[10] Furthermore, the residual spectrum comprises a second broader component that is probably not associated to surface-modified bulk states but to the presence of either anisotropic surface overlayer[28] or to surface roughness.[29]

Optical structure is also observed around the E_0'-triplet that originates in a linear-strain effect. Furthermore, since the E_2 band is close in energy to the E_0'-triplet, from Fig. 1 alone it is difficult to make a conclusion about whether it does or does not contribute to the RD line shape. However, as discussed below, additional polarized photoreflectance measurements show that the optical response of the E_2 band is largely isotropic, thus leading to a negligible contribution to the RD line shape.

From the above discussion we may conclude that RD lines shapes around the E_0-triplet are simpler than the corresponding photoreflectance (PR) or spectroscopic ellipsometry (SE) spectra that comprise transitions from all, isotropic and anisotropic, critical points. In particular we note that while E_2 band dominates both SE and PR lines shapes, it does not appreciably contribute to RD spectra.

To remove the intrinsic component of the RD spectra of Figs. 1(a) and 1(c), given by the spectrum of Fig. 1(b), we subtracted spectrum (c) from spectrum (a) and divided the result by 2. The RD spectrum obtained in this way is shown with open circles in Fig. 2. This spectrum, as already mentioned, is dominated by transitions of Λ and Γ symmetry. We note the vertical offset in the difference spectrum that makes

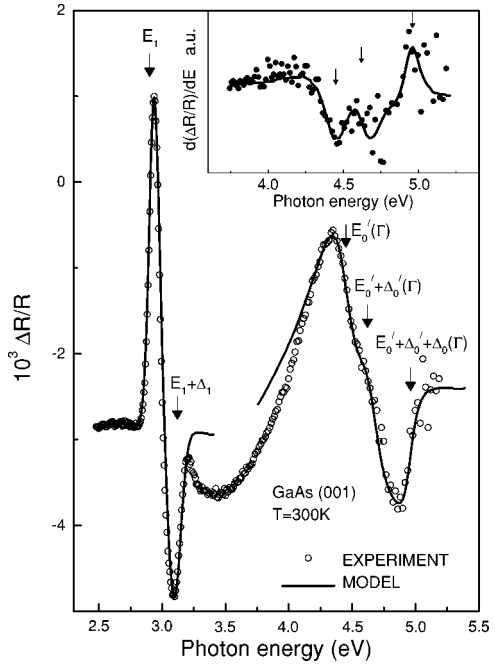

FIG. 2. RD spectrum obtained by subtracting spectrum (c) from spectrum (a) of Fig. 1. The solid lines correspond to the calculated spectrum obtained using Eqs. (3), (5)–(7), and (2). Inset shows the first energy derivatives of the RD experimental spectrum and its fitted line shape. Arrows indicate the energy positions for the interband GaAs bulk transitions.

it negative, except around E_1. This offset probably results from nonresonant contributions to sample reflectance anisotropy. In order to have a theoretical model for this line shape, in the next section we develop expressions for the change in dielectric function due to the applied uniaxial strain for the electronic transitions of Λ and Γ symmetry. Continuous lines in Fig. 2 are fits to the experimental RD spectrum obtained from the developed theoretical line-shape model.

IV. THEORY

In what follows we will consider a (001)-oriented zinc-blende semiconductor with an uniaxial stress applied along [110] direction. This stress induces a strain with nonzero tensor components given by[30]

$$e_{xx} = e_{yy} = \frac{S_{11} + S_{12}}{2} X, e_{zz} = S_{12} X,$$

$$e_{xy} = e_{yx} = \frac{S_{44}}{4} X, \tag{1}$$

where X is the strength of the applied stress, and S_{11}, S_{12}, and S_{44} are the elastic compliance modulii.

The deformation tensor (1) induces a change $\Delta\varepsilon$ in the dielectric function. We define this change by the subtraction of the dielectric function for $[1\bar{1}0]$ polarization from the dielectric function for [110] polarization. The RD spectrum is related to this change according to[31]

$$\frac{\Delta R}{R} = \mathrm{Re}[(\alpha - i\beta)\Delta\varepsilon], \tag{2}$$

where α and β are Seraphin coefficients. To obtain an expression for $\Delta\varepsilon$ we must calculate the energy shifts and the interband square matrix elements as a function of tensor (1) for each electronic transition.

We will consider in this section the contribution of the points of Λ and Γ symmetry to the RD spectrum.

A. Points of Λ symmetry

Under a stress along [110], transitions E_1 and $E_1+\Delta_1$ split apart into two sets of four equivalent points in the Brillouin zone: a first set containing ellipsoids along [111], $[\bar{1}\bar{1}1]$, $[1\bar{1}\bar{1}]$ and $[\bar{1}1\bar{1}]$, and a second set containing points along $[\bar{1}11]$, $[11\bar{1}]$, $[1\bar{1}1]$, and $[\bar{1}\bar{1}\bar{1}]$.[27] Using the energy shifts and the matrix elements for a stress along [110] as reported elsewhere,[27] the change in dielectric function for transitions of Λ symmetry is given by

$$\Delta\varepsilon' = \frac{1}{E^2}\frac{\partial E^2 \varepsilon'(E, E_1 + \delta E_{so} + \delta E_h')}{\partial E}\delta E_s' + \frac{4r\gamma'}{\Delta_1}\varepsilon'(E, E_1 + \delta E_{so} + \delta E_h'), \tag{3}$$

where Δ_1 is the spin orbit splitting energy for valence band, $r=+1(-1)$ refers to E_1 $(E_1+\Delta_1)$, and

$$\delta E_{so} = (1-r)\frac{\Delta_1}{2},$$

$$\delta E_s' = \frac{D_1^5 S_{44}}{4\sqrt{3}} X,$$

$$\delta E_h' = \frac{D_1^1 (S_{11} + 2S_{12})}{\sqrt{3}} X,$$

$$\gamma' = \frac{D_5 S_{44}}{2\sqrt{6}} X, \tag{4}$$

where D_1^5 and D_1^1 are the interband orthorhombic and hydrostatic deformation potential for transitions of Λ symmetry, respectively. D_5 is the orthorhombic deformation potential for the valence band. To obtain Eq. (3) we have assumed that $\gamma \gg \delta E_s'$, where γ is the broadening parameter for the interband transitions.

B. Points of Γ symmetry

Interband transitions corresponding to points of Γ symmetry are shown in Fig. 3. These transitions are E_0', $E_0'+\Delta_0'$, and $E_0'+\Delta_0'+\Delta_0$, corresponding to transitions $\Gamma_8^v \rightarrow \Gamma_7^c$, $\Gamma_8^v \rightarrow \Gamma_8^c$, and $\Gamma_7^v \rightarrow \Gamma_8^c$, respectively.[17,18]

Under the effect of the applied stress the Γ_8 levels split and consequently each transition splits into two components as shown in Fig. 3. Thin and thick arrows in this figure correspond to transitions E_0' and $E_0'+\Delta_0'+\Delta_0$, respectively.

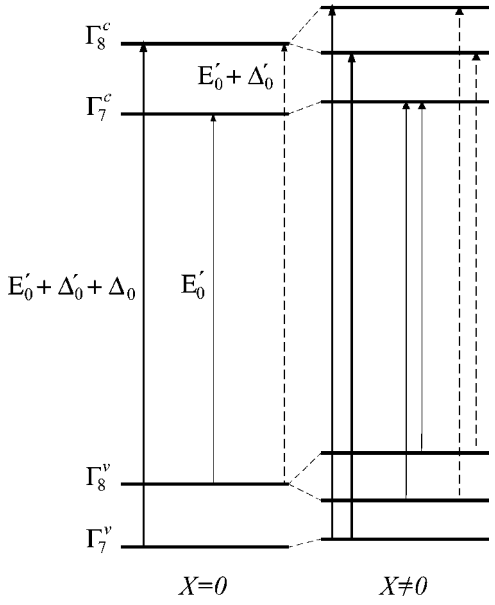

FIG. 3. Energy levels for critical points of Γ symmetry with and without applied stress. Each bulk transition splits into a doblet due to cubic symmetry break down. For each transition the two splitted transitions are indicated by E_0' (thin lines), $E_0'+\Delta_0'$ (dashed lines), and $E_0'+\Delta_0'+\Delta_0$ (thick lines).

Note that while the valence band splits for transition E_0', it is the conduction band that splits for transition $E_0'+\Delta_0'+\Delta_0$. We show also in Fig. 3 with dashed arrows the two components of the $E_0'+\Delta_0'$ transition. Note that for this last transition both bands split.

We calculated the change in dielectric function for each critical point by using Eqs. (A6)–(A9) in the Appendix. Assuming that $\gamma \gg \Delta E^{i,j}$, where γ is the broadening parameter of the interband transitions, and by further neglecting the quadratic component of the energy shifts in Eqs. (A6) and (A8), we have for E_0', $E_0'+\Delta_0'$ and $E_0'+\Delta_0'+\Delta_0$, respectively,

$$\Delta\varepsilon'' = \frac{3}{8E^2}\frac{dE^2\varepsilon''}{dE}(\delta E_{0,1}^2 + 3\delta E_{1,1}^2)^{1/2} + \frac{3}{2}\frac{\delta E_{1,2}}{\delta_2}\varepsilon'', \quad (5)$$

$$\Delta\varepsilon''' = \left\{ \frac{2-\sqrt{6}}{8}\left[\frac{\delta E_{0,1}}{\delta_1} + \frac{\delta E_{0,2}}{\delta_2} \right] - 3\frac{2+\sqrt{6}}{8}\left[\frac{\delta E_{1,1}}{\delta_1} + \frac{\delta E_{1,2}}{\delta_2} \right] \right\}\varepsilon''', \quad (6)$$

$$\Delta\varepsilon'''' = -\frac{3}{8E^2}\frac{dE^2\varepsilon''''}{dE}(\delta E_{0,2}^2 + 3\delta E_{1,2}^2)^{1/2} + \frac{3}{2}\frac{\delta E_{1,1}}{\delta_1}\varepsilon'''', \quad (7)$$

where ε'', ε''', and ε'''' stand, respectively, for the contribution of E_0', $E_0'+\Delta_0'$ and $E_0'+\Delta_0'+\Delta_0$ to the overall dielectric function ε. Parameters $\delta E_{i,j}$ are proportional to the deformation potentials of the valence and conduction bands, and δ_1 and δ_2 are the spin orbit splitting energies for valence and conduction bands, respectively. All parameters in Eqs. (5)–(7) are defined in Sec. VIII. Note that for E_0' and $E_0'+\Delta_0'+\Delta_0$ transitions the components proportional to the first energy derivative of ε have opposite signs. We also note that transition $E_0'+\Delta_0'$ has only a component proportional to ε'''.

V. DISCUSSION

To calculate the Λ component of the RD spectrum we have deconvoluted the contributions of critical points E_1 and $E_1+\Delta_1$ to the overall dielectric function. The deconvolution was carried out by fitting Lorentzian line shapes to the real and imaginary parts of the experimental dielectric function spectra, following the procedure described elsewhere.[26] With these fits and the first energy-derivative of the dielectric function, Eqs. (2) and (3) allowed us to calculate the solid line spectrum in Fig. 2 around E_1 and $E_1+\Delta_1$ energies. To calculate the RD line shape we have used the parameters: $S_{11}=0.117\,562\times10^{-11}$ cm^2/dyn, $S_{12}=-0.036\,5132\times10^{-11}$ cm^2/dyn, $S_{44}=0.168\,35\times10^{-11}$ cm^2/dyn for the elastic compliance constants,[32] $\Delta_1=0.22$ eV,[18] for the split-off energy and $D_1^1=-8.4$ eV,[33] $D_5=-5.0$ eV,[33] and $D_1^5=8.8$ eV,[30] for the deformation potentials. The strength of the stress was taken as a fitting parameter obtaining the value $X=-1.5\times10^9$ dyn/cm^2, in good agreement with the value of $X=-1.4\times10^9$ dyn/cm^2 determined from the used calibrated spring. We note that to take account for the nonresonant contributions to the reflectance anisotropy, we downward shifted the calculate spectra by 2.9×10^{-3}. The same downward shift was applied to the E_0'-triplet fit discussed below.

Carrying out a similar deconvolution for the contributions of the E_0'-triplet to the overall dielectric function poses some difficulties due to the fact that the E_0' and $E_0'+\Delta_0'$ transitions of Γ symmetry are separated for only 50 meV from their Δ-symmetry partners.[17] Furthermore, the $E_0'+\Delta_0'+\Delta_0$ transition is only 120 meV away from the dominating E_2 band and appears only as a small shoulder.[17,18] To overcome this problem we have instead modeled the contributions ε'', ε''', and ε'''' of the $E_0'(\Gamma)$-triplet with three, excitonic-type, Lorentzian line shapes located at the reported critical point energies: $E_0'(\Gamma)=4.45$ eV, $E_0'+\Delta_0'(\Gamma)=4.62$ eV, and $E_0'+\Delta_0'+\Delta_0=4.95$ eV.[17] We have further used the known 4:2:1 ratio for the amplitudes of the components of the $E_0'(\Gamma)$-triplet (i.e., the amplitude of the $E_0'+\Delta_0'+\Delta_0$ transition is four times weaker than that of E_0').[17,34]

At this stage it is necessary to address the point relative to the contribution of the E_2 band to the RD line shape. This is a crucial issue as the E_2 band dominates the GaAs reflectance spectrum around 5.0 eV. We note that on the basis of symmetry arguments alone we may expect such a contribution to exist, since the E_2 band is believed to comprise transitions of Σ symmetry that respond anisotropically to the applied uniaxial strain. To settle this point we performed photoreflectance (PR) measurements with both unpolarized light and with light polarized along [110]. PR measurements were carried out with the technique reported elsewhere.[26] Taking into account that the piezoelectric strain induced by the surface electric field has the same symmetry[26] as that of the tensor given in Eq. (1), we may expect PR spectra to exhibit a polarization anisotropy. Results are shown in Fig. 4 for a *n*-type GaAs(001) sample with a doping level of 1.0

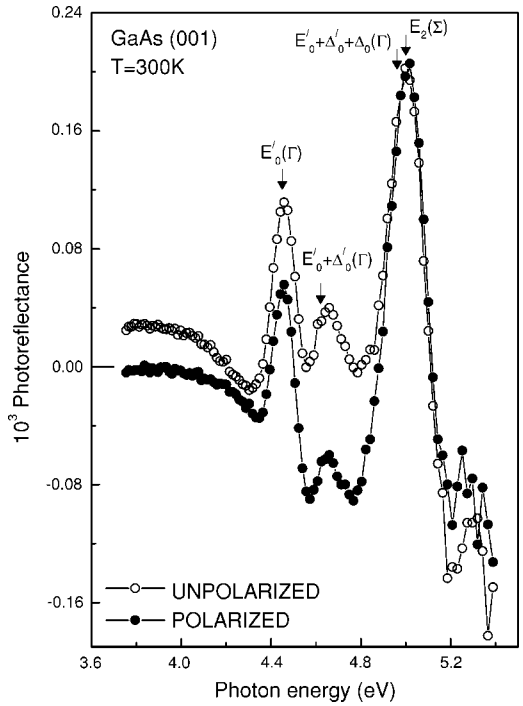

FIG. 4. PR spectra at room temperature for unpolarized probe light (open circles) and for probe light polarized along the [110] direction (solid circles). Note that for energies higher than 4.9 eV the PR line shape depends weakly on polarization. For energies lower than 4.9 eV the PR line-shape dependence on polarization is evident.

$\times 10^{18}$ cm^{-3}. Open circles correspond to unpolarized light and solid circles to [110] polarization. From Fig. 4 it is clear that while the reflectance response of the E_0'-triplet is anisotropic, the response of the dominating E_2 band is largely isotropic, independent of the polarization. We may thus conclude that the contribution of the E_2 band to the RD line shape is negligible. This conclusion is further supported by the fact that, as discussed below, we obtain an excellent fit to the RD experimental line shape in the energy range from 3.8−5.2 eV, solely on the basis of the anisotropic response of the E_0'-triplet.

By using the line shapes for ε'', ε''', and ε'''' and Eqs. (5)–(7) we obtained the fitted RD line shape given by the solid line around 4.5 eV in Fig. 2. We have used phases and broadening energies of the Lorenzian line shapes as fitting parameters. We have further used the following literature parameter values: $a'=-2.5$ eV[35] for the hydrostatic deformation potential, $b=-2.2$ eV, $d=-5.4$ eV,[32] for the valence band and $b^c=1.6$ eV and $d^c=-5.5$ eV[35] for the conduction band. With filled circles in the inset of Fig. 2 we show, in the energy range around E_0'-triplet, the first energy-derivative of the RD experimental spectrum, along with the energy-derivative of the corresponding fit (continuous line). As it can be seen from Fig. 2, the experimental RD spectrum can be adequately fitted by the model developed here.

We note that the spectral structure of the RD line shape of Fig. 2 is qualitatively similar to that reported previously for strains of piezoelectric origin; i.e., it shows a maximum around E_1 and a minimum around $E_1+\Delta_1$.[26] As a matter of fact, the theoretical RD line shape for piezoelectric strains reported previously[26] is a special case (zero-trace strain tensor) of the more general RD line shape presented in this paper.

VI. CONCLUSIONS

We have measured the RD spectrum for GaAs(001) under [110] and [1$\bar{1}$0] uniaxial stresses. RDS measurements were carried out in the energy range from 2.5−5.2 eV that includes transitions of Λ, Γ, Δ, X, and Σ symmetries. The RD spectrum is found to comprise only Λ-symmetry and Γ-symmetry transitions whereas Δ, X critical points remain isotropic under the applied stress and the Σ transition contribution results negligible. The measured RD spectrum shows sharp structure around E_1 and $E_1+\Delta_1$ critical points (Λ-symmetry) as well as in the energy interval corresponding to the E_0'-triplet (Γ-symmetry), that are due to a linear-strain effect. We have further developed a strain related RD line-shape model that includes both Λ and Γ critical point contributions. The theoretical model is in excellent agreement with the measured RD spectrum. Results presented in this paper should probe to be useful in the identification of strain-related features in RD spectra. We further hope that this paper will contribute to the understanding of the different physical mechanisms leading to reflectance anisotropies in zinc-blende semiconductors.

ACKNOWLEDGMENTS

The authors wish to thank E. Ontiveros and G. Rodríguez-Pedroza for technical assistance. This work was supported by Consejo Nacional de Ciencia y Tecnologia through Grant Nos. 41248-F and 485100-5-33976E, and FAI-UASLP under Contract Nos. C02-FAI-11-18.79 and C03-FAI-11-18.53.

APPENDIX

The unperturbed wave functions of Γ_8 and Γ_7 symmetries are given, respectively, by[30]

$$|3/2,3/2\rangle = \frac{1}{\sqrt{2}}(\tilde{X}+i\tilde{Y})|\tilde{\uparrow}\rangle,$$

$$|3/2,-1/2\rangle = \frac{1}{\sqrt{6}}[2\tilde{Z}|\tilde{\downarrow}\rangle + (\tilde{X}-i\tilde{Y})|\tilde{\uparrow}\rangle], \tag{A1}$$

$$|1/2,-1/2\rangle = \frac{1}{\sqrt{3}}[\tilde{Z}|\tilde{\downarrow}\rangle - (\tilde{X}-i\tilde{Y})|\tilde{\uparrow}\rangle], \tag{A2}$$

where

$$\tilde{X} = -Z, \tilde{Y} = (Y-X)/\sqrt{2},$$

$$\tilde{Z} = (Y+X)/\sqrt{2}, \tag{A3}$$

and

$$|\tilde{\uparrow}\rangle = e^{-i\pi/8}|\uparrow\rangle/\sqrt{2} + e^{i\pi/8}|\downarrow\rangle/\sqrt{2},$$

$$|\tilde{\downarrow}\rangle = -e^{-i\pi/8}|\uparrow\rangle/\sqrt{2} + e^{i\pi/8}|\downarrow\rangle/\sqrt{2}. \tag{A4}$$

To calculate the effects on the energy levels and interband square matrix elements produced by the strain of Eq. (1) we have used the perturbative Pikus-Bir Hamiltonian:[30]

$$H^{(i)} = -a^{(i)}(S_{11}+2S_{12})X - 3b^{(i)}\left[\left(L_x^2-\frac{1}{3}L^2\right)\frac{S_{11}+S_{12}}{2}X + \left(L_y^2-\frac{1}{3}L^2\right)\frac{S_{11}+S_{12}}{2}X + \left(L_z^2-\frac{1}{3}L^2\right)S_{12}X\right] - \frac{\sqrt{3}}{4}d^{(i)}(L_xL_y+L_yL_x)S_{44}X, \tag{A5}$$

where $a^{(i)}$, $b^{(i)}$, and $d^{(i)}$ are the hydrostatic, tetragonal, and orthorhombic deformation potentials, respectively, and i is the band index. L_x, L_y, and L_z are the components of the angular momentum. In the next two sections we calculate, by using Eqs. (A1)–(A5), the shifts of the energy levels and the square matrix elements for Γ-symmetry transitions.

E_0' and $E_0'+\Delta_0'+\Delta_0$ transitions

Thin and dashed arrows in Fig. 3 correspond to transitions E_0' and $E_0'+\Delta_0'+\Delta_0$, respectively. Both transitions connect states of Γ_7 and Γ_8 symmetry.[17] Under the strain given by Eq. (1) the states split into two levels and consequently both E_0' and $E_0'+\Delta_0'+\Delta_0$ transitions split into doublets as shown in Fig. 3.

We define the parameters $\delta E_h = a'(S_{11}+2S_{12})X$, $\delta E_{0,1} = 2b(S_{11}-S_{12})X$, $\delta E_{1,1} = dS_{44}X/\sqrt{3}$, and $\delta_1 = \Delta_0$ for valence band and $\delta E_{0,2} = 2b^c(S_{11}-S_{12})X$, $\delta E_{1,2} = d^cS_{44}X/\sqrt{3}$, and $\delta_2 = \Delta_0'$ for conduction band, where b and b^c are the tetragonal deformation potentials for valence and conduction bands, respectively, and d and d^c are the orthorhombic deformation potentials for valence and conduction bands, respectively. Δ_0 and Δ_0' are the the spin orbit splitting energies for valence and for conduction bands, respectively.

The energy shifts for the doublet components of transitions E_0' and $E_0'+\Delta_0'+\Delta_0$ (that will be labeled **a** and **b**) are given by

$$\Delta E_{\mathbf{a}}^{i,j} = \delta E_h + \frac{1}{4}(j-i)(\delta E_{0,i}^2+3\delta E_{1,i}^2)^{1/2} - \frac{3}{8}(j-i) \times\left(\frac{1}{4}\frac{(\delta E_{0,i}-\delta E_{1,i})^2}{\delta_i} + \frac{\delta E_{0,j}^2+3\delta E_{1,j}^2}{3\delta_j}\right), \tag{A6}$$

$$\Delta E_{\mathbf{b}}^{i,j} = \delta E_h - \frac{1}{4}(j-i)(\delta E_{0,i}^2+3\delta E_{1,i}^2)^{1/2} - \frac{3}{8}(j-i) \times\left(\frac{1}{12}\frac{(\delta E_{0,i}+3\delta E_{1,i})^2}{\delta_i} + \frac{\delta E_{0,j}^2+3\delta E_{1,j}^2}{3\delta_j}\right),$$

where $i=1, j=2$ stand for E_0' and $i=2, j=1$ for $E_0'+\Delta_0'+\Delta_0$. Note that the energy shifts for E_0' and $E_0'+\Delta_0'+\Delta_0$ have opposite signs [through the factor $(j-i)$], whenever the deformation potentials d and d^c have the same sign.

The square interband transition matrix elements are

$$M_{\mathbf{a}}^{\mathbf{u}} = \frac{1}{4}\left[1+\frac{\delta E_{0,j}+3\delta E_{1,j}}{2\delta_j}\right]M_0,$$

$$M_{\mathbf{a}}^{\mathbf{v}} = \left[1-\frac{\delta E_{0,j}+3\delta E_{1,j}}{4\delta_j}\right]M_0,$$

$$M_{\mathbf{b}}^{\mathbf{u}} = \frac{3}{4}\left[1-\frac{\delta E_{0,j}-\delta E_{1,j}}{2\delta_j}\right]M_0,$$

$$M_{\mathbf{b}}^{\mathbf{v}} = 0, \tag{A7}$$

where M_0 is the unperturbed square transition matrix element and **u** and **v** indicate polarizations along [110] and $[1\bar{1}0]$, respectively.

$E_0'+\Delta_0'$ transition

The $E_0'+\Delta_0'$ transition connects two states of Γ_8 symmetry, as it is illustrated by dashed arrows in Fig. 1. Under the strain given by Eq. (1), both conduction and valence bands splits into two levels leading to double transition bands. The energy shifts for this two bands are given by

$$\Delta E_{\mathbf{c}}^{i,j} = \delta E_h - \frac{1}{4}(j-i)[(\delta E_{0,i}^2+3\delta E_{1,i}^2)^{1/2}+(\delta E_{0,j}^2+3\delta E_{1,j}^2)^{1/2}] - \frac{1}{32}(j-i)\left(\frac{(\delta E_{0,i}+3\delta E_{1,i})^2}{\delta_i} - 3\frac{(\delta E_{0,j}-\delta E_{1,j})^2}{\delta_j}\right), \tag{A8}$$

where $i=1$, $j=2$ stand for one band and $i=2$, $j=1$ for the other.

The square matrix elements are given by:

$$M_{\mathbf{c}}^{\mathbf{u}} = \frac{3}{2}\left[\frac{1}{3}+\frac{1}{4}\frac{\delta E_{0,i}-\delta E_{1,i}}{\delta_i} - \frac{1}{12}\frac{\delta E_{0,j}+3\delta E_{1,j}}{\delta_j}\right]M_0,$$

$$M_{\mathbf{c}}^{\mathbf{v}} = \frac{3}{2}\left[\frac{1}{3}+\frac{1}{6}\frac{\delta E_{0,j}+3\delta E_{1,j}}{\delta_j}\right]M_0. \tag{A9}$$

In Sec. IV we have used Eqs. (A6)–(A9), to model the several Γ contributions to the RD spectrum as explained in the main text.

*Electronic address: lflm@cactus.iico.uaslp.mx

[1] D. E. Aspnes and A. A. Studna, Phys. Rev. Lett. **54**, 1956 (1985).
[2] Z. Sobiesierski, D. I. Westwood, and C. C. Matthai, J. Phys. C **10**, 1 (1998); N. Esser, W. G. Schmidt, C. Cobet, K. Fleischer, A. Shkrebtii, C. O. Fimland, and W. Richter, J. Vac. Sci. Technol. B **19**, 1756 (2001); F. Arciprete, C. Goletti, E. Placidi, P. Chiaradia, M. Fanfoni, F. Patella, C. Hogan, and A. Balzarotti, Phys. Rev. B **68**, 125328 (2003).
[3] D. E. Aspnes, J. P. Harbison, A. A. Studna, L. T. Florez, and K. Kally, J. Vac. Sci. Technol. B **6**, 1127 (1988); D. E. Aspnes, E. Colas, A. A. Studna, R. Bhat, M. A. Koza, and V. G. Keramidas, Phys. Rev. Lett. **61**, 2782 (1988).
[4] Takashi Kita, Osamu Wada, T. Nakayama, and M. Murayama, Phys. Rev. B **66**, 195312 (2002); M. Pristovsek, S. Tsukamoto, B. Han, J.-T. Zettler, and W. Richter, J. Cryst. Growth **248**, 254 (2003).
[5] Itaru Kamiya, D. E. Aspnes, L. T. Florez, and J. P. Harbison, Phys. Rev. B **46**, 15 894 (1992).
[6] M. J. Begarney, L. Li, C. H. Li, D. C. Law, Q. Fu, and R. F. Hicks, Phys. Rev. B **62**, 8092 (2000); Akihiro Ohtake and Nobuyuki Koguchi, Appl. Phys. Lett. **83**, 5193 (2003).
[7] W. G. Schmidt, F. Bechstedt, K. Fleischer, C. Cobet, N. Esser, W. Richter, J. Bernholc, and G. Onida, Phys. Status Solidi A **188**, 1401 (2001).
[8] S. Visbeck, T. Hannappel, M. Zorn, J. T. Zettler, and F. Willig, Phys. Rev. B **63**, 245303 (2001); K. Hingerl, R. E. Balderas-Navarro, W. Hilber, A. Bonanni, and D. Stifter, *ibid.* **62**, 13 048 (2000).
[9] L. F. Lastras-Martínez, D. Rönnow, P. V. Santos, M. Cardona, and K. Eberl, Phys. Rev. B **64**, 245303 (2001).
[10] L. F. Lastras-Martínez and A. Lastras-Martínez, Solid State Commun. **98**, 479 (1996); L. F. Lastras-Martínez and A. Lastras-Martínez, Phys. Rev. B **54**, 10 726 (1996).
[11] L. F. Lastras-Martínez and A. Lastras-Martínez, Phys. Rev. B **64**, 085309 (2001).
[12] R. E. Balderas-Navarro, K. Hingerl, A. Bonanni, H. Sitter, and D. Stifter, Appl. Phys. Lett. **78**, 3615 (2001); Y. H. Chen, Z. G. Wang, J. J. Qian, and Z. Yang, J. Appl. Phys. **88**, 1695 (2000).
[13] W. L. Mochán and R. G. Barrera, Phys. Rev. Lett. **55**, 1192 (1985).
[14] S. E. Acosta-Ortíz and A. Lastras-Martínez, Solid State Commun. **64**, 809 (1987); S. E. Acosta-Ortíz and A. Lastras-Martínez, Phys. Rev. B **40**, 1426 (1989).
[15] D. Rönnow, L. F. Lastras-Martínez, M. Cardona, and P. V. Santos, J. Opt. Soc. Am. A **16**, 568 (1999).
[16] L. F. Lastras-Martínez, R. E. Balderas-Navarro, M. Chavira-Rodríguez, J. M. Flores-Camacho, and A. Lastras-Martínez, Phys. Status Solidi B **240**, 500 (2003).
[17] D. E. Aspnes and A. A. Studna, Phys. Rev. B **7**, 4605 (1973).
[18] P. Lautenschlager, M. Garriga, S. Logothetidis, and M. Cardona, Phys. Rev. B **35**, 9174 (1987).
[19] L. F. Lastras-Martínez, A. Lastras-Martínez, and R. E. Balderas-Navarro, Rev. Sci. Instrum. **64**, 2147 (1993).
[20] K. Sangwal, in *Defects in Solids*, edited by S. Amelinckx and J. Nihoul (North-Holland, Amsterdam, 1987), Vol. 15, p. 427.
[21] D. E. Aspnes and A. A. Studna, Appl. Opt. **14**, 220 (1975).
[22] R. M. A. Azzam and N. M. Bashara, *Ellipsometry and Polarized Light* (North-Holland, Amsterdam, 1997).
[23] G. E. Jellison, Jr., Opt. Mater. (Amsterdam, Neth.) **1**, 151 (1992).
[24] D. E. Aspnes, G. P. Schwartz, G. J. Gualtieri, A. A. Studna, and B. Schwartz, J. Electrochem. Soc. **128**, 590 (1981).
[25] E_2 is commonly accepted to be formed by a dominant transition of Σ symmetry and four weaker transitions of X symmetry. These last four do not contribute to reflectance anisotropy.
[26] A. Lastras-Martínez, R. E. Balderas-Navarro, L. F. Lastras-Martínez, and M. A. Vidal, Phys. Rev. B **59**, 10 234 (1999).
[27] L. F. Lastras-Martínez, M. Chavira-Rodríguez, A. Lastras-Martínez, and R. E. Balderas-Navarro, Phys. Rev. B **66**, 075315 (2002).
[28] D. E. Aspnes, J. Vac. Sci. Technol. B **3**, 1498 (1985).
[29] D. E. Aspnes, Phys. Rev. B **41**, 10 334 (1990).
[30] F. H. Pollak and M. Cardona, Phys. Rev. **172**, 816 (1968).
[31] D. E. Aspnes, in *Handbook on Semiconductors*, edited by M. Balkanski (North-Holland, Amsterdam, 1980), Vol. 2, p. 121.
[32] *Elements and III-V Compounds*, edited by O. Mandelung, M. Schultz and H. Weiss, Landolt-Börnstein, New Series, Vol. III/17a (Springer-Verlag, Berlin, 1982).
[33] P. Etchegoin, J. Kircher, M. Cardona, C. Grein, and E. Bustarret, Phys. Rev. B **46**, 15 139 (1992).
[34] D. E. Aspnes, Phys. Rev. Lett. **28**, 913 (1972).
[35] A. Blacha, H. Presting, and M. Cardona, Phys. Status Solidi B **126**, 11 (1984).